Available online at www.sciencedirect.com
ScienceDirect
Trans. Nonferrous Met. Soc. China 21(2011) 604−611
Transactions of Nonferrous Metals Society of China
www.tnmsc.cn

Effect of atomic structure on migration characteristic and solute segregation of ordered domain interfaces formed in $Ni_{75}Al_xV_{25-x}$

ZHANG Ming-yi[1], CHEN Zheng[1], WANG Yong-xin[1], MA Guang[2], LU Yan-li[1], FAN Xiao-li[1]

1. State Key Laboratory of Solidification Processing, Northwestern Polytechnical University, Xi'an 710072, China;
2. Northwest Institute for Nonferrous Metal Research, Xi'an 710016, China

Received 1 April 2010; accepted 27 August 2010

Abstract: Based on the microscopic phase-field model, ordered domain interfaces formed between $D0_{22}$ (Ni_3V) phases along [001] direction in $Ni_{75}Al_xV_{25-x}$ alloys were simulated, and the effects of atomic structure on the migration characteristic and solute segregation of interfaces were studied. It is found that the migration ability is related to the atomic structure of interfaces, and three kinds of interfaces can migrate except the interface (001)//(002) which has the characteristic of $L1_2$ (Ni_3Al) structure. V atoms jump to the nearest neighbor site and substitute for Ni, and vice versa. Because of the site selectivity behaviors of jumping atoms, the number of jumping atoms during the migration is the least and the jumping distance of atoms is the shortest among all possible modes, and the atomic structures of interfaces are unchanged before and after the migration. The preferences and degree of segregation or depletion of alloy elements are also related to the atomic structure of interface.

Key words: atomic migration characteristic; solute segregation; site selectivity; microscopic phase-field; ordered domain interface

1 Introduction

The goal of interface science is to facilitate material manufacture of technological importance by optimizing the properties of materials based on a comprehensive understanding of the microstructure of the interface and its influence on material performances[1]. As a kind of buried structures in material, interface is also much more difficult to investigate than other microstructures of materials. Molecular dynamics[2], Monte Carlo[3] and phase field[4] methods have been the useful atomistic simulation methods for exploring the solid interface behaviors today, such as the connection among atomic interface structure, interface migration[5] and interface property[6]. However, the understanding of the basic atomic mechanism associated with interface migration remains rudimentary for many factors may affect the dynamics and kinetic property of interfaces. It was reported that the interface mobility is strongly dependent on misorientation, which is attributed to both the interface structure and segregation[7]. The interface migration mechanism not only depends on the crystallography misorientation of the adjacent grains[8], driving force of the interface migration[9], interface geometries[10], etc., but also may change in the process of migration[11]. Today, atomistic simulation studies have facilitated the understanding of complex behavior of interfaces, especially in the area that experimental techniques is still problematic to investigate.

Recently, the microscopic phase-field model has been used to study the migration characteristic of interfaces during the precipitation process of nickel based alloy, and it is found that the migration ability and composition of interface can be affected by the atomic structure as well[12]. Compared with some of the atomistic simulation which should assume the atomic structure of the studied interface prior[13], this method not only can trace the atomic migration during the interface migration but also can obtain the information of microstructure evolution without any prior assumption. In the present work, the atomic structure, migration process, and compositions of ordered domain interfaces formed between $D0_{22}$ phases along [001] direction during the precipitation process of $Ni_{75}Al_xV_{25-x}$ alloys were investigated using the microscopic phase-field model.

Foundation item: Projects (50941020, 10902086, 50875217, 20903075) supported by the National Natural Science Foundation of China; Projects (SJ08-ZT05, SJ08-B14) supported by the Natural Science Foundation of Shaanxi Province, China; Project (CX200905) supported by the Doctorate Foundation of Northwestern Polytechnical University, China
Corresponding author: ZHANG Ming-yi; Tel: +86-29-88474095; E-mail: zmy1688@gmail.com
DOI: 10.1016/S1003-6326(11)60757-7

2 Microscopic phase-field model

Microscopic phase-field model, based on the microscopic diffusion equations which are the discrete lattice form of the Cahn-Hilliard equations, was first proposed by KHACHATURYAN[14] and developed by PODURI and CHEN[15] for the ternary alloy system. The equations for ternary alloy systems are

$$\begin{cases}\dfrac{\mathrm{d}P_{\mathrm{A}}(r,t)}{\mathrm{d}t}=\dfrac{1}{k_{\mathrm{B}}T}\sum_{r'}\left[L_{\mathrm{AA}}(r-r')\dfrac{\partial F}{\partial P_{\mathrm{A}}(r',t)}+L_{\mathrm{AB}}(r-r')\dfrac{\partial F}{\partial P_{\mathrm{B}}(r',t)}\right]\\ \dfrac{\mathrm{d}P_{\mathrm{B}}(r,t)}{\mathrm{d}t}=\dfrac{1}{k_{\mathrm{B}}T}\sum_{r'}\left[L_{\mathrm{BA}}(r-r')\dfrac{\partial F}{\partial P_{\mathrm{A}}(r',t)}+L_{\mathrm{BB}}(r-r')\dfrac{\partial F}{\partial P_{\mathrm{B}}(r',t)}\right]\end{cases} \tag{1}$$

and for ternary systems, $P_{\mathrm{C}}(r,\ t)=1-P_{\mathrm{A}}(r,\ t)-P_{\mathrm{B}}(r,\ t)$, where $P_{\alpha}(r,\ t)$ (α=A, B or C) represents the probability of finding an α atom at a given lattice site r at a given time t which is a reduced time; $L_{\alpha\beta}(r-r')$ (α and β=A, B or C) is the kinetic coefficients proportional to the probability of elementary diffusion jumps from site r to r' per unit time; and F is the total Helmholtz free energy of the system based on the mean-field approximation, which can be written as a function of single site occupation probability:

$$\begin{aligned}F=&-\frac{1}{2}\sum_{r}\sum_{r'}\left[V_{\mathrm{AB}}(r-r')P_{\mathrm{A}}(r)P_{\mathrm{B}}(r')+\right.\\&V_{\mathrm{BC}}(r-r')P_{\mathrm{B}}(r)P_{\mathrm{C}}(r')+V_{\mathrm{AC}}(r-r')P_{\mathrm{A}}(r)P_{\mathrm{C}}(r')\left.\right]+\\&k_{\mathrm{B}}T\sum_{r}\left[P_{\mathrm{A}}(r)\ln(P_{\mathrm{A}}(r))+\right.\\&\left.P_{\mathrm{B}}(r)\ln(P_{\mathrm{B}}(r))+P_{\mathrm{C}}(r)\ln(P_{\mathrm{C}}(r))\right]\end{aligned} \tag{2}$$

where the effective pair interaction $V_{\alpha\beta}$ is deduced from the pair interaction $\omega_{\alpha\beta}$.

With the atomic pair interactions as the only inputs and without any prior assumption concerning the atomic structure of ordered phases, the model can describe the ordering, phase separation, growth and coarsening process of ordered phases simultaneously within the same formalism, and can produce crystallographic structures of various possible ordered phases and atomic configurations by minimizing the total energy of the alloy system. Studies show that the applications of microscopic phase-field model in the studies of the phase transformation and coarsening process of ordered phases in binary and ternary alloy systems show excellent agreement both with experiment results and other simulation results[16−17].

3 Results and discussion

3.1 Atomic structure and migration characteristic of interfaces

$D0_{22}$ (Ni_3V) phase precipitates in the aging process of $Ni_{75}Al_xV_{25-x}$ alloy when the Al content of alloy is low. Schematic diagrams of the $D0_{22}$ crystal structure of Ni_3V and the projection of $D0_{22}$ (Ni_3V) structure along [010] direction are shown in Figs.1(a) and (b), respectively.

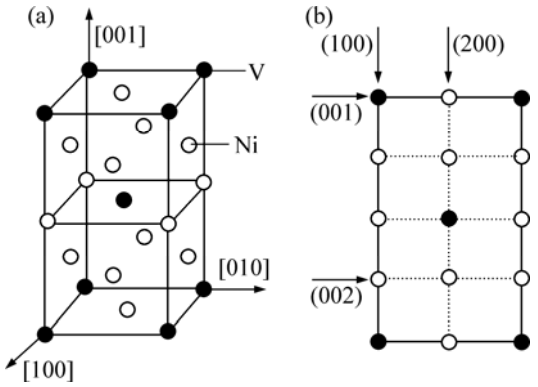

Fig.1 Schematic diagrams of crystal structure of $D0_{22}$ (a) and its projection along [010] direction (b)

Fig.2 shows the atomic microstructure evolution of $Ni_{75}Al_3V_{22}$ alloy precipitated at 1 150 K. In the simulated pictures, the black sites represent Ni and form a background; the gray sites represent V, and the higher the site occupation probability of V, the darker the gray level. The Al sites present to be white. By analyzing the atomic arrangement of interface using the atomic microstructure evolution picture and the site occupation probability of alloy elements on the site of interfaces, it is found that there are three kinds of interfaces formed between $D0_{22}$ phases along [001] direction in Fig.2. Arrows A and B in Fig.2(a) denote the same kind of interface (002)//(002), arrow C denotes the interface (002)//(002)$\cdot^{1/2}$[100], and arrow D denotes the interface (001)//(002). As Fig.2 shown, interface (002)//(002)$\cdot^{1/2}$[100] and interface (002)//(002) migrate during the microstructure evolution. The $L1_2$ phase is precipitated at the interface (001)//(002) as the arrow E indicated in Fig.2(c), which can be attributed to characteristic of $L1_2$ (Ni_3Al) structure for interface (001)//(002).

Fig.3 shows the atomic microstructure evolution of $Ni_{75}Al_{6.5}V_{18.5}$ alloy precipitated at 1 185 K. The interface denoted by arrow A in Fig.3(a) is also the interface (001)//(002). It is found that $L1_2$ phase does not precipitate at interface (001)//(002) during the microstructure evolution. However, when the interface denoted by arrow B does not migrate, the interface (001)//(002) stands still, but it disappears when the interface denoted by arrow C migrates, as shown in Figs.3(c). Then, we concluded that the interface (001)//(002) cannot migrate by itself, and the migration ability is related to the atomic structure of interfaces. Another kind of interface formed between $D0_{22}$ phases

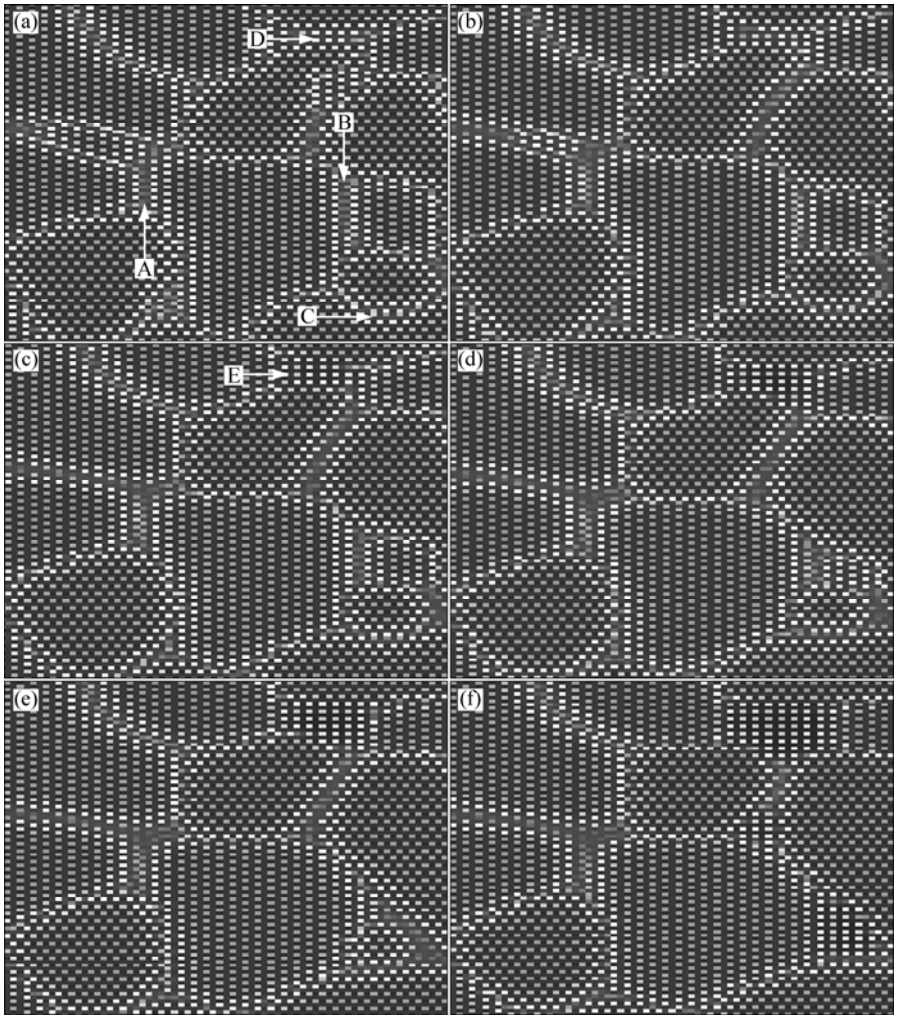

Fig.2 Atomic microstructure evolution pictures of $Ni_{75}Al_3V_{22}$ alloy precipitated at 1 150 K (arrows A and B indicate interface (002)// (002), arrow C indicates interface (002)// $(002)\cdot^{1/2}$[100], arrow D indicates interface (001)//(002)): (a) *t*=40 000; (b) *t*=50 000; (c) *t*=60 000; (d) *t*=70 000; (e) *t*=80 000; (f) *t*=100 000

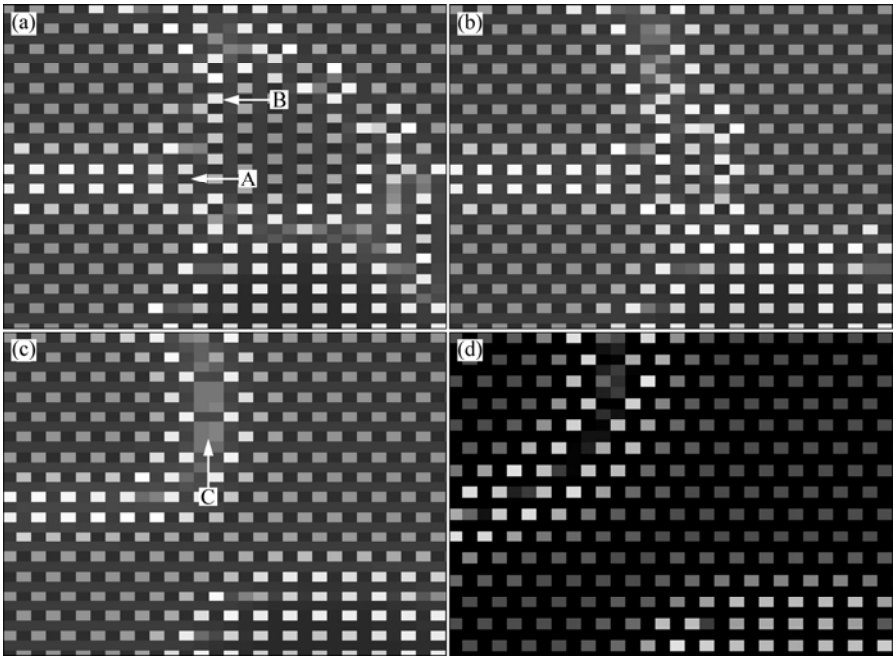

Fig.3 Atomic microstructure evolution pictures of $Ni_{75}Al_{6.5}V_{18.5}$ alloy precipitated at 1 185 K (arrow A indicates interface (001)// (002)): (a) *t*=200 000; (b) *t*=260 000; (c) *t*=27 000; (d) *t*=300 000

along [001] direction is found during the precipitation process of $Ni_{75}Al_{7.5}V_{17.5}$ alloy at 1 100 K, as shown in Fig.4. The interface (001)//(001)·$^{1/2}$[100], denoted by arrow A in Fig.4(a), can migrate during the microstructure evolution. Figs.5(a)−(d) show the schematic diagrams of the atomic structure of interface (002)//(002)·$^{1/2}$[100], (002)//(002), (001)//(002), (001)//(001)·$^{1/2}$[100], respectively. For the convenience of discussion, numbers 1−6 are labeled at the sites of interfaces.

According the atomic microstructure evolution pictures, it can be found that the jump of atoms shows site selectivity behaviors during the migration of interfaces, each interface which can migrate has its own atom jump mode. To verify the atom jump mode of each interface, the site occupation probability evolution of Ni and V at the sites labeled by 1−6 is shown in Fig.6. Fig.6(a) shows the site occupation probability evolution of Ni and V at sites 1 and 2 at interface (002)//(002)·$^{1/2}$[100]. The site occupation probability of V at the site 1 decreases and the site occupation probability of V at the site 2 increases at the same time. The site occupation probabilities of V at sites 1 and 2 show symmetrical but contrary evolutions, the same as site occupation probability evolution of Ni. Then it is believed that, during the migration of interface (002)//(002)·$^{1/2}$[100], the V atoms at sites 1 jump to the nearest sites labeled by 2 to substitute for Ni atoms, and at the same time, the Ni atoms on sites 2 jump to the nearest sites labeled by 1 to substitute for V atoms. It is the exchange of the V on the site 1 and the Ni on the site 2 to induce the migration of interface (002)//(002)·$^{1/2}$[100]. According to Figs.6(b) and (c), it can be concluded that the V atoms on the site 3 exchange with the Ni atoms at the site 4 during the migration process of interface (002)//(002), and the V atoms at the site 5 exchange with the Ni atoms on the site 6 during the migration process of interface (001)//(001)·$^{1/2}$[100]. It should be noticed that after the exchange of the Ni and V atoms, the atomic structure of interfaces retains the same, which can be attributed to the site selectivity behavior of V during the interface migration.

By analyzing the atom jump mode of the interface which can migrate itself, it can be found that the V atoms exchange with the Ni atoms at the nearest neighbor sites, i.e. the jump of atoms shows site selectivity behaviors during the migration. It also can be found that, among all the possible atomic jump modes which may induce the migration of interfaces, the number of atoms needed to jump during the migration is the least. That is to say, the atom jump mode to induce the migration of interfaces is the way of least resistance. Notice that the atomic structures of all the studied interfaces retain the same before and after the migration. Then, it is easy to understand why the atoms show site selectivity behavior during the interface migration. It is the atomic site selectivity behaviors that make the atomic structures of interfaces retain the same before and after the migration,

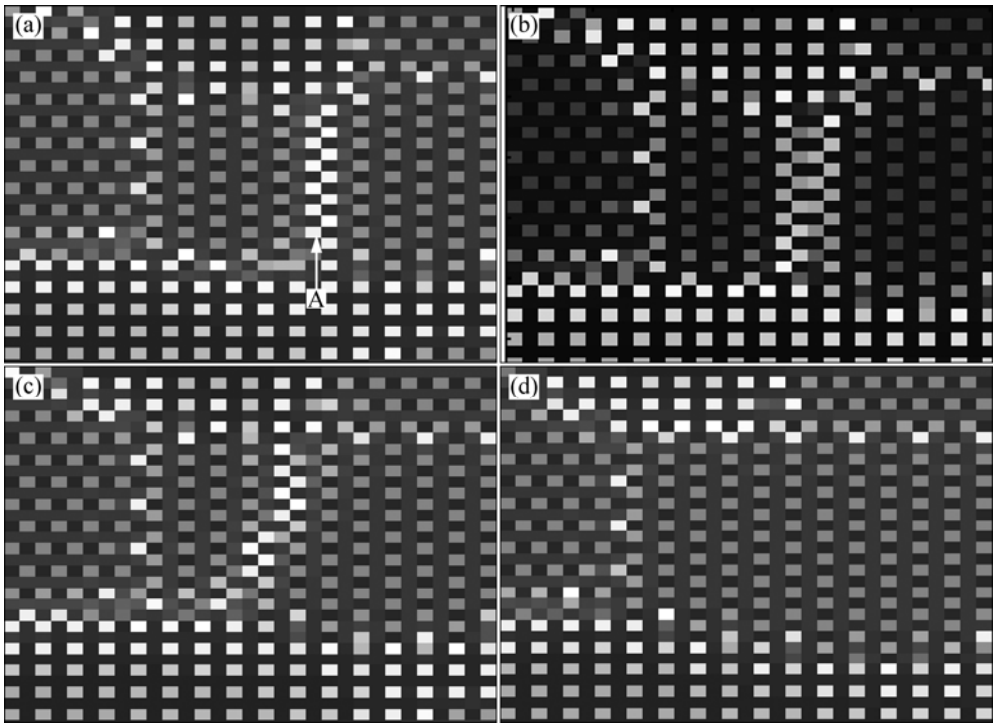

Fig.4 Atomic microstructure evolution pictures of $Ni_{75}Al_{7.5}V_{17.5}$ alloy precipitated at 1 100 K (arrow A indicates interface (001)//(001)·$^{1/2}$[100]): (a) t=130 000; (b) t=145 000; (c) t=200 000; (d) t=300 000

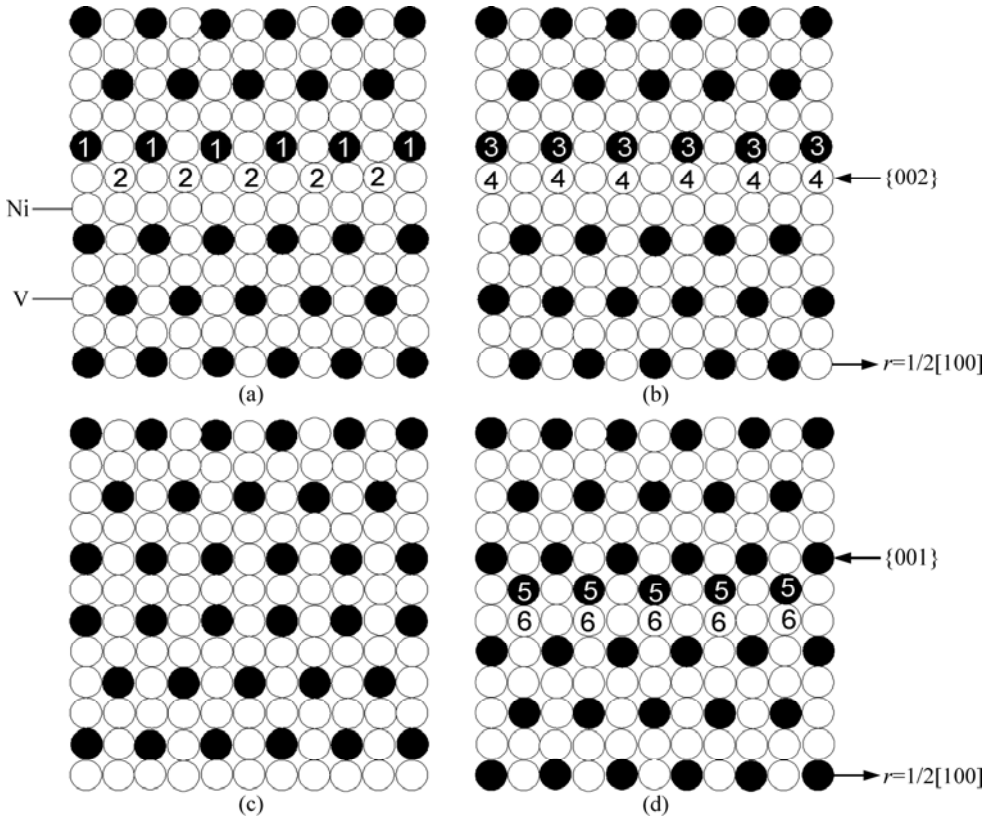

Fig.5 Schematic diagrams of atomic structure of interfaces: (a) (002)//(002); (b) (002)//(002)·$^{1/2}$[100]; (c) (001)//(002); (d) (001)//(001)·$^{1/2}$[100]

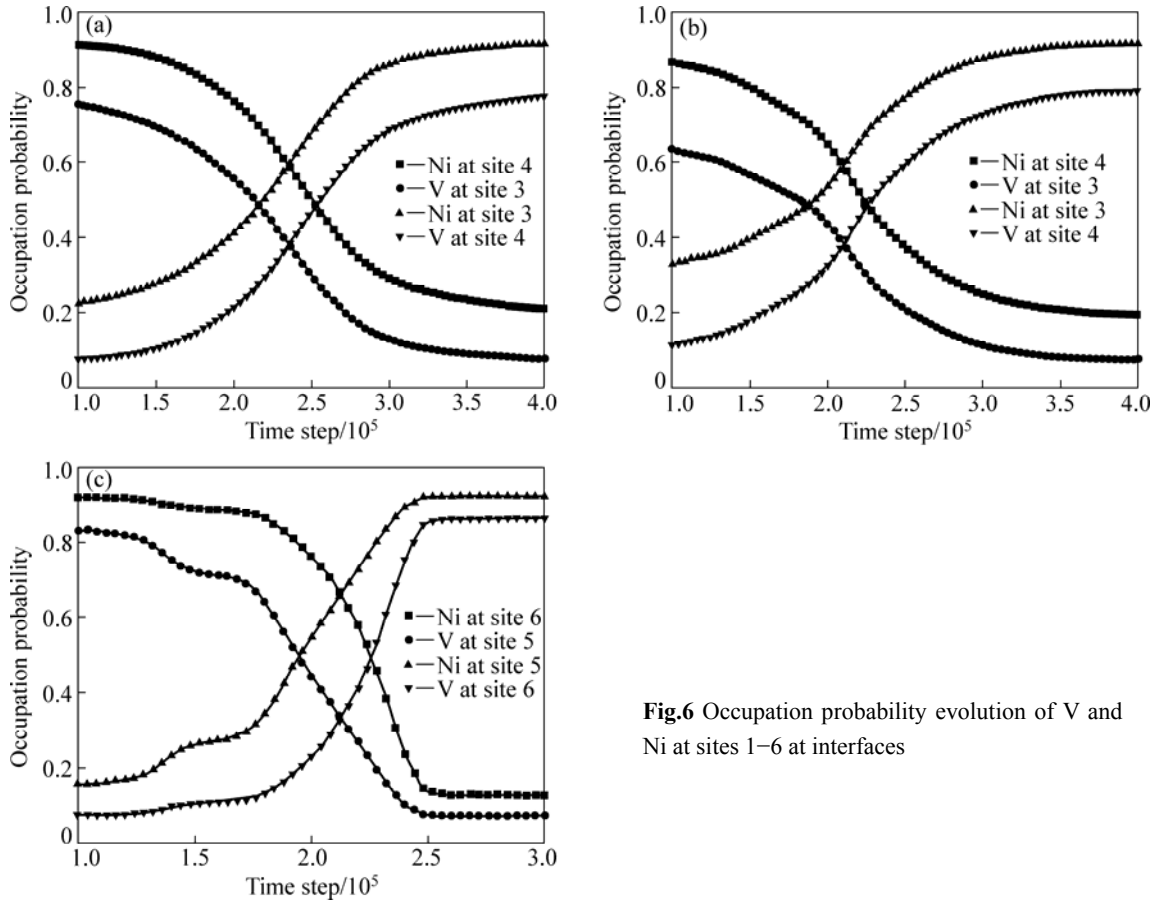

Fig.6 Occupation probability evolution of V and Ni at sites 1−6 at interfaces

and the interface energy remains the same before and after the migration. But in long views, the interface area and also the interface energy would decrease with the migration of interface, and supply the driving force of interface migration. In one word, the atom jumps select the optimist way in the aspect of kinetics and thermodynamic to induce the migration of interfaces.

3.2 Solute segregation and depletion of interfaces

The distributions of alloy elements, represented by the average site occupation probabilities of alloy elements, across the interfaces are shown in Fig.7. The compositions of interfaces (002)//(002)·$^{1/2}$[100] and (002)//(002) are calculated during the precipitation process of $Ni_{75}Al_3V_{22}$ alloy at 1 150 K, the compositions of interface (001)//(002) are calculated during the precipitation process of $Ni_{75}Al_{6.5}V_{18.5}$ alloy at 1 185 K, and the compositions of interface (001)//(001)·$^{1/2}$[100] are calculated during the precipitation process of $Ni_{75}Al_{7.5}V_{17.5}$ alloy at 1 100 K. The concentrations of alloy elements at the interfaces are different from those inside the domains. At the same interface, the alloy elements have different preferences of segregation or depletion. At all the four kinds of studied interfaces, Ni segregates and V depletes. However, Al depletes at the interface (001)//(001)·$^{1/2}$[100] but segregates at the other three kinds of interfaces. The segregation of Al and the precipitation of $L1_2$ phase at the interface (001)//(002) show excellent agreement with previous study[18]. By analyzing the atomic structure of the four kinds of interfaces, it can be found that there is no Ni atom plane at the interfaces (001)//(001)·$^{1/2}$[100] while the interfaces (002)//(002)·$^{1/2}$[100] and (002)//(002) both have two Ni atom planes, and there is one Ni atom plane at the interface (001)//(002). That may be the reason of the difference of segregation and depletion preference of Al at the studied four kinds of interfaces.

The concentration of Al at interface (001)//(002) is obviously higher than at the other interfaces, since the interface (001)//(002) has the characteristic of $L1_2$ (Ni_3Al) structure. Under the same condition, the concentrations of Ni and Al at interface (002)//(002) are higher than those at interface (002)//(002)·$^{1/2}$[100] and the concentration of V at interface (002)//(002) is lower than that at interface (002)//(002)·$^{1/2}$[100] as shown in Figs.7(a) and (b). Previous study had shown that the site preference of alloy elements affects the solute segregation at interface[19]. The difference of atomic

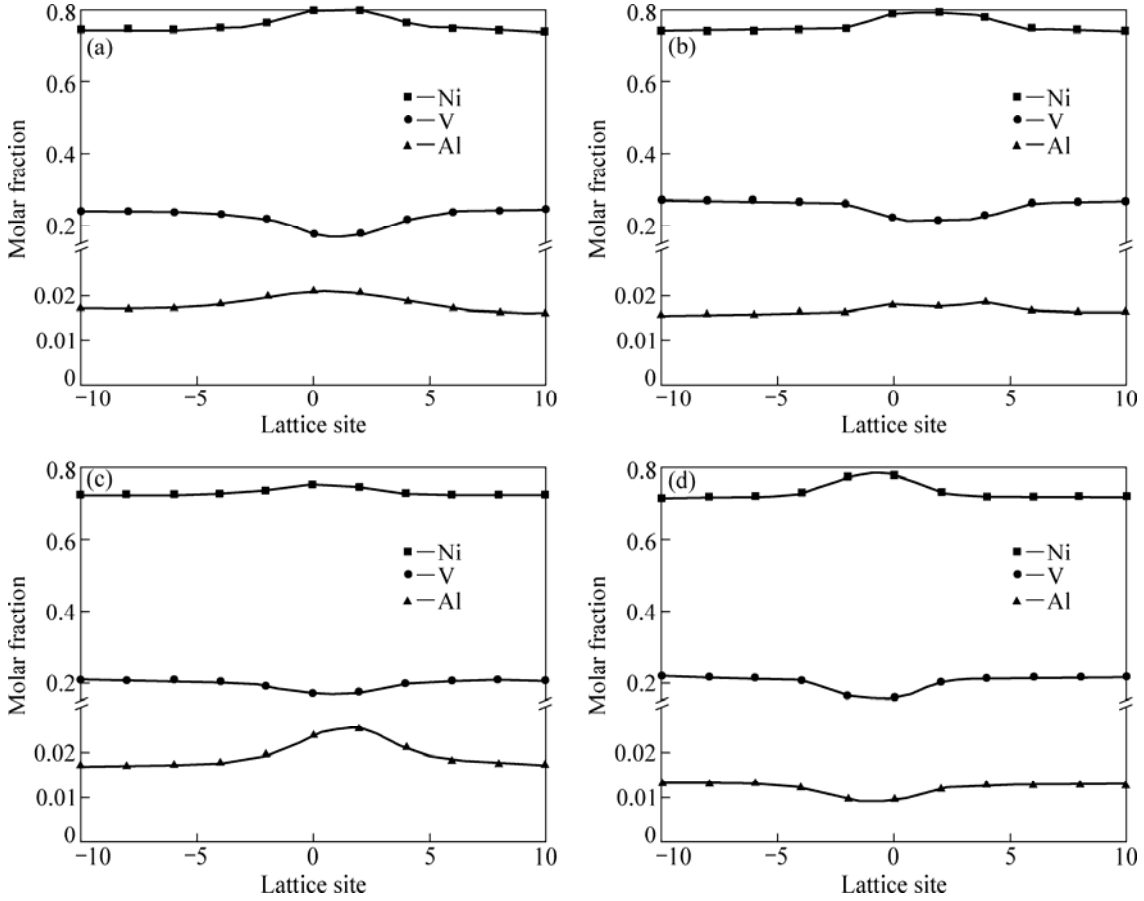

Fig.7 Distribution of alloy elements across interfaces: (a) (002)//(002); (b) (002)//(002)·$^{1/2}$[100]; (c) (001)//(002); (d) (001)//(001)·$^{1/2}$[100]

structure between the interface (002)//(002) and (002)//(002)·$^{1/2}$[100] may also affect the site preference of alloy elements, and then affect the degree of solute segregation and depletion. Further study will be carried out to study the relationship between the atomic environment, site preference and solute segregation.

4 Conclusions

1) Four kinds of interfaces are formed between $D0_{22}$ phases along [100] direction in $Ni_{75}Al_xV_{25-x}$. Not all the interfaces can migrate during the evolution of microstructure, and the migration ability is related to the atomic structure of interface. Except the interface (001)//(002) which has the characteristic of $L1_2$ (Ni_3Al) structure, the other three kinds of interfaces can migrate during the microstructure evolution, and the $L1_2$ phase can be easily precipitated at the interface (001)//(002).

2) V atoms show a site selectivity behavior during interface migration, and jump to the nearest neighbor site and substitute for Ni, and vice versa. The site selectivity behaviors of atoms force the atomic structures of interfaces retain the same before and after the migration. The jump and substitution mode of atoms may be the optimization way in thermodynamics and kinetics for interface migration because the number of jumping atoms during migration is the least and the jumping distance of atoms is the shortest among all the possible modes.

3) The preferences and degrees of solute segregation or depletion are different at different interfaces. At all the studied interfaces, Ni segregates and V depletes; Al depletes at the interface (001)//(001)·$^{1/2}$[100] but segregates at the other three kinds of interfaces. The concentration of Al at the interface (001)//(002) is the highest because the interface (001)//(002) has the characteristic of $L1_2$ (Ni_3Al) structure.

References

[1] WANG S Q, YE H Q. Theoretical studies of solid-solid interfaces [J]. Curr Opin Solid State Mater Sci, 2006, 10(1): 26−32.

[2] ZHOU L, ZHOU N, SONG G. Collective motion of atoms in grain boundary migration of a bcc metal [J]. Philosophical Magazine A, 2006, 86(36): 5885−5895.

[3] BOS C, SOMMER F, MITTEMEIJER E J. An atomistic analysis of the interface mobility in a massive transformation [J]. Acta Mater, 2005, 53(20): 5333−5341.

[4] GRONHAGEN K, JOHN A. Grain-boundary segregation and dynamic solute drag theory—A phase-field approach [J]. Acta Mater, 2007, 55(3): 955−960.

[5] UPMANYU M, HASSOLD G N, KAZARYAN A, HOLM E A, WANG Y, PATTON B, SROLOVITZ D J. Boundary mobility and energy anisotropy effects on microstructural evolution during grain growth [J]. Interface Sci, 2002, 10(2): 201−216.

[6] OGUMA R, EGUCHI T, MATSUMURA S, SON S K. Domain growth and off-phase boundary structures in $L1_2$-type ordering [J]. Acta Mater, 2006, 54(6): 1533−1539.

[7] GOTTSTEIN G, MOLODOV D A, WINNING M, SHIVINDLERMAN L S. Grain boundary dynamics: A novel tool for microstructure control [J]. Interface Sci, 2001, 9(2): 297−306.

[8] GOTTSTEIN G, MOLODOV D A, SHIVINDLERMAN L S, SROLOVITZ D J, WINNING M. Grain boundary migration: misorientation dependence [J]. Curr Opin Solid St M, 2001, 5(1): 9−14.

[9] ZHANG H, MENDELEV M I, SROLOVITZ D J. Computer simulation of the elastically driven migration of a flat grain boundary [J]. Acta Mater, 2004, 52(9): 2569−2576.

[10] BERNSTEIN N. The influence of geometry on grain boundary motion and rotation [J]. Acta Mater, 2008, 56(5): 1106−1113.

[11] CAHN J W, MISHIN Y, SUZUKI A. Coupling grain boundary motion to shear deformation [J]. Acta Materi, 2006, 54(19): 4953−4975.

[12] ZHANG M Y, CHEN Z, WANG Y X, LU Y L, ZHANG L P, ZHAO Y. Simulation of ordered domain interfaces formed between $L1_2$ phases in Ni-Al-V alloy using microscopic phase-field model [J]. Acta Metallurgica Sinica, 2007, 43(10): 1101−1106.

[13] GONG H R, LIU B X. Influence of interfacial texture on solid-state amorphization and associated asymmetric growth in immiscible Cu-Ta multilayers [J]. Physical Review B, 2004, 70(10): 134202.

[14] KHACHATURYAN A G. Theory of structural transformations in solids [M]. New York: Wiley, 1983: 23−26.

[15] PODURI R, CHEN L Q. Computer simulation of atomic ordering and compositional clustering in the pseudobinary Ni_3Al-Ni_3V system [J]. Acta Mater, 1998, 46(5): 1719−1729.

[16] PAREIGE C, BLAVATTE D. Simulation of the FCC-FCC+$L1_2$+$D0_{22}$ kinetic reaction [J]. Scripta Mater, 2001, 44(2): 243−247.

[17] LU Y L, CHEN Z, WANG Y X. Microscopic phase-field simulation of the early precipitation mechanism of Ni_3Al phase in Ni-Al alloys [J]. Mater Lett, 2008, 62(8−9): 1385−1388.

[18] BENDERSKY L A, BIANCANIELLO F S, WILLIAMS M E. Evolution of the two-phase microstructure $L1_2$+$D0_{22}$ in near-eutectoid Ni_3(Al, V) alloy [J]. J Mater Res, 1994, 9(12): 3068−3082.

[19] KITASHIMA T, YOKOKAWA T, YEH A C, HARADA H. Analysis of element content effects on equilibrium segregation at γ/γ' interface in Ni-based superalloys using the cluster variation method [J]. Intermetallics, 2008, 16(6): 779−784.

$Ni_{75}Al_xV_{25-x}$合金中有序畴界结构对界面迁移特征和溶质偏聚的影响

张明义[1]，陈 铮[1]，王永欣[1]，马 光[2]，卢艳丽[1]，范晓丽[1]

1. 西北工业大学 凝固技术重点实验室，西安 710072；
2. 西北有色金属研究院，西安 710016

摘 要：基于微观相场模型，通过分析 $Ni_{75}Al_xV_{25-x}$合金在沉淀过程中 $D0_{22}$ (Ni_3V)相沿[001]方向形成的有序畴界面的界面结构、界面迁移及界面成分，研究界面结构对界面迁移特征和溶质偏聚的影响。研究表明：$D0_{22}$相沿[100]方向形成 4 种有序畴界，界面的迁移性与界面结构有关，除具有 $L1_2$相的局部特征的界面(001)//(002)之外，其余 3 种界面都可以迁移；在界面的迁移过程中，V 原子跃迁至最近邻的 Ni 位置并置换 Ni 原子，反之亦然，即处在最近邻的 Ni 原子和 V 原子发生位置交换而导致界面迁移；在迁移过程中，原子的跃迁行为具有位置选择性，每种可迁移界面都按照特定的原子跃迁模式进行迁移；原子在跃迁过程中选择最优化的路径使得界面发生迁移，原子跃迁过程中的位置选择性使得界面在迁移前、后的结构保持不变；合金元素在界面处具有不同的贫化和偏聚倾向，在所有的界面处，Ni 偏聚而 V 贫化，Al 在界面(001)//(001)·$^{1/2}$[100]处贫化在其他界面处偏聚；同种合金元素在不同界面处的偏聚和贫化程度不同。

关键词：界面迁移特征；溶质偏聚；位置选择性；微观相场；有序畴界

(Edited by YANG Hua)